A Study on the Improvement of the Performance of Power Amplifiers by Defected Ground Structure

Jong-Sik Lim[1] · Young-Taek Lee[1] · Jun-Seok Park[2] · Dal Ahn[2] · Jae-Hee Han[1] · Byung-Sung Kim[3] · Sang-wook Nam[1]

Abstract

This paper describes the improvement in performance of power amplifiers by Defected Ground Structure (DGS) for several operating classes. Due to its excellent capability of harmonic rejection, DGS plays a great role in improving the main performance of power amplifiers such as output power, power added efficiency, harmonic rejection, and intermodulation distortion (IMD3). In order to verify the improvement in performance of power amplifiers by DGS, measured data for a 30 Watts power amplifier with and without DGS attached under several operating classes are illustrated and compared. The principle of the performance improvement is described with simple Volterra nonlinear transfer functions. Also, the measured performance for two cases, i.e. with and without DGS, and the quantities of improvement for the various operating classes are compared and discussed.

Ⅰ. Introduction

The most important design targets of power amplifiers are high output power, efficiency, and good linearity. One of methods to improve the output power is to tune the harmonics at the output[1]~[3]. Among the harmonics, the second harmonic is especially in want of tuning, because its magnitude is relatively larger than other harmonics. Previous techniques for tuning harmonics include adding a $\lambda/4$ short-circuited stub[2]~[5] and using a chip capacitor with self-resonance near the second harmonic[6]. Radisic et al. pointed out that the above techniques are narrow band and presented a new method using photonic bandgap (PBG) structure at the output of the power amplifier[7]. Improvement in performance of the power amplifier was achieved, but drilling a lot of holes and adding copper tape onto the ground plane are required in realizing PBG.

Recently, a new technique for harmonic tuning using microstrip line with Defected Ground Structure (DGS) at the output has been proposed[8]. DGS is also a kind of periodic structure. However it is much easier to fabricate, because DGS patterns are realized when the amplifier circuit is etched at the same time. Due to its effective additional L-C components[9], DGS has a specified passband with ultra low loss and very wide stopband characteristics, and does not show the periodic passband property. If this passband is overlapped to the operating frequency band of a power amplifier, the property of DGS is very important in rejecting harmonics, because DGS can tune not only the second, but also the third and fourth harmonics of power amplifiers[8], while the technique using PBG tunes the second harmonic only[7]. The excellent rejection of the second harmonic plays a great positive role in improving the main performance of power amplifiers such as output power, power added efficiency, harmonic rejection, and linearity.

In order to verify the improvement in performance by DGS, a 30 Watts level power amplifier has been fabricated and measured at 2.11~2.17 GHz for two cases, i.e. the power amplifier with DGS at the output section ("WITH DGS") and the power amplifier without DGS ("WITHOUT DGS"). The test items for comparison in this work are output power, the second and third harmonic powers, power added efficiency, power gain, and the third order intermodulation distortion (IMD3). Measurements have been performed for various operating classes by adjusting the initial drain current (IdsQ) with input power swept. The measured data for the two cases will be described and compared with simple Volterra nonlinear transfer functions.

Ⅱ. The Microstrip Line with DGS on the Ground Plane

Fig. 1 shows the general structure of the microstrip line with DGS proposed in[8],[9]. The transfer characteristics of this transmission line, which depends on the dimensions of the

Manuscript received August 7, 2001; revised October 15, 2001.

[1] School of Electrical Engineering, Seoul National University
[2] Division of Information Technology Engineering, SoonChunHyang University
[3] School of Electrical and Computer Engineering, SungKyunKwan University

dumb-bell shaped DGS pattern and periodic distance, is just like a low pass filter performance which is also shown in PBG[7]. An important difference in transfer performance between the PBG in [7] and DGS in [8] is that DGS has a very wide stopband, and no periodic passband exists. This means that DGS can suppress the higher order harmonics as well as the second harmonic, while PBG only rejects the second harmonic. Theoretically and practically, it is desirable to reject the third and fourth harmonics at the output even though they are relatively small compared to the second harmonic. Because the related theory and measured characteristics of the microstrip with DGS have been introduced well in [10], it is not described in detail here.

The purpose of using DGS in this work is to improve the performance of power amplifiers by tuning the harmonics. In order to obtain this goal using the minimum number of DGS patterns, two unit patterns are selected. It is required that the DGS have low loss in the passband and excellent rejection at harmonic bands. If the straight microstrip line with DGS has some loss at the operating frequency of the power amplifier, it is required to compensate for the width of microstrip line, as in this work, to get low loss at the operating band and high rejection at harmonic band. In practice, another advantage of the compensated microstrip with DGS is that the width of the microstrip line is much wider than that of the conventional microstrip line for the same characteristic impedance due to the increased effective inductive component[8]~[10]. This is a great advantage in application where very high power is handled. Therefore, it is recommended to compensate for the line width to get low loss at the passband and high rejection at harmonic bands when DGS is used in several tens of Watt-level power amplifiers.

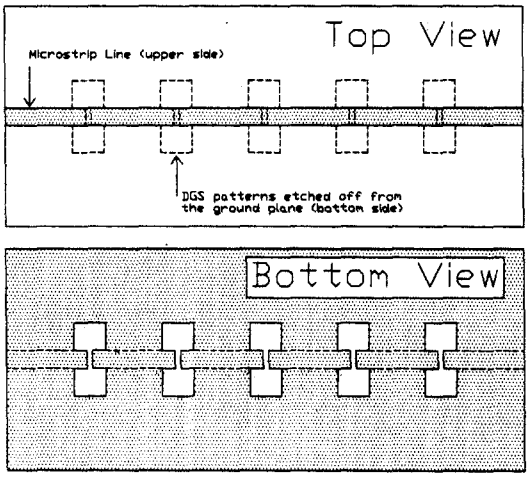

Fig. 1. General structure of the microstrip line with DGS patterns ("DGS line") on the ground plane.

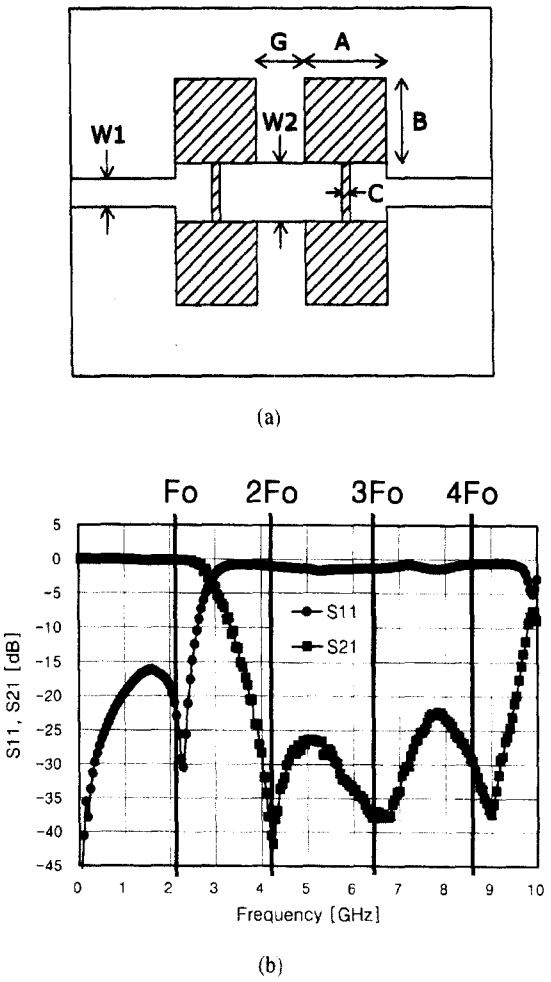

Fig. 2. (a) The microstrip line with two DGS patterns and compensated width and (b) its measured performance.

Fig. 2 (a) shows the compensated width of microstrip line when there are two DGS patterns, and Fig. 2 (b) illustrates the measured property on the substrate with 3.48 of dielectric constant and 30 mils of thickness. The dimensions are A=B=5 mm, C=0.5 mm, G=3 mm, W1=1.7 mm, and W2=3.5 mm. W1 is the width of the 50-Ω microstrip line for connection.

The measured data shown in Fig. 2(b) shows a typical property of a low pass filter (LPF), though it was not intended to design a LPF. The clear differences between the DGS line and the conventional LPF are ; 1) much steeper cutoff, 2) much wider width of microstrip line, in other words, no need for a very high impedance line, 3) much smaller size, and so on.

The measured low loss of 0.15 dB at 2.14 GHz means that DGS at the output of the amplifier rarely reduce linear gain. On the contrary, it should be noted that the slope of the cut-off is very steep and the rejections at the second, third, and fourth

harmonic frequencies are very excellent. Therefore, it is possible to tune the harmonics, while the PBG structure rejects only the second harmonic because of periodic passband characteristics.

Ⅲ. Power Amplifier and 1-Tone Measurement

We adopted a 30 Watts device to build a power amplifier as shown in Fig. 3 (a). Two quarter-wave lines with high impedance are used for bias supply. Even though these lines act like a $\lambda/4$ short-circuited stub for tuning the second harmonic to some extent, it is not sufficient in high power amplifiers over Watt-level. In practice, the considerable second harmonic power has been measured during power sweep in the case of "WITHOUT DGS".

The key concept of this work is shown in Fig. 3 (b). The fundamental (Fo) and harmonic components (nFo, n=2,3,....) at the output of the power amplifier are faced with DGS line. Only the fundamental component passes to the final output section, while harmonics are reflected back into the device. This causes the fundamental power to increase[4]. Currently, the DGS line is separated from the amplifier for the measurement for the two cases, but this can be solved easily by merging it into the output section of the amplifier.

Fig. 4 (a) shows the measured output power at fundamental and power added efficiency (PAE) for the two cases under the IdsQ of 400 mA, which is close to class AB operation, as an example. It is evident that output power and efficiency have been improved by adopting DGS. The improved power gain by DGS is 0.37~0.75 dBm, which corresponds to the increase by 0.1~1.3 watts. The improvement of PAE is also considerable. Fig. 4 (a) shows that the improved PAE by DGS is 0.56~3.4 %.

The reduction of the second harmonic component is more

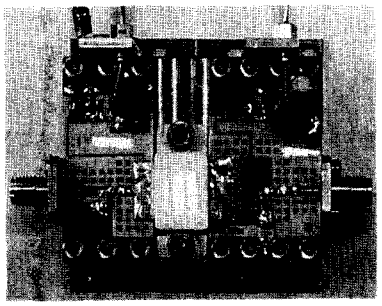

(a)

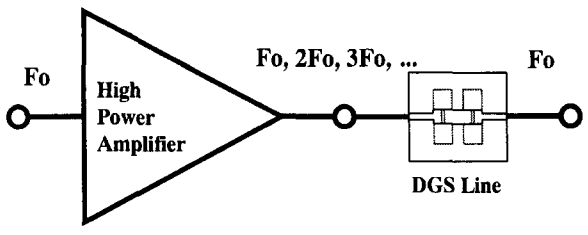

(b)

Fig. 3. (a) The fabricated 30 Watts power amplifier.
(b) The power amplifier combined with DGS line.

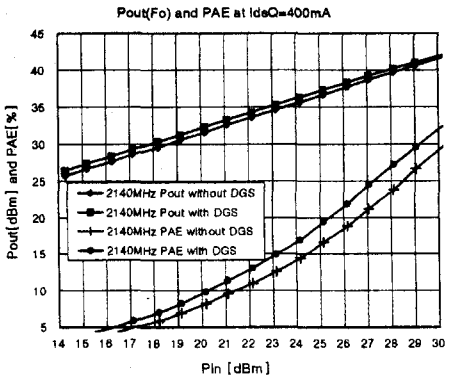

(a)

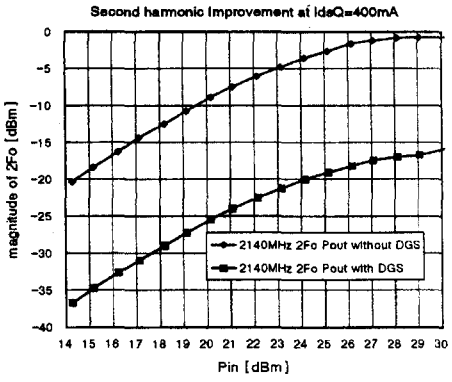

(b)

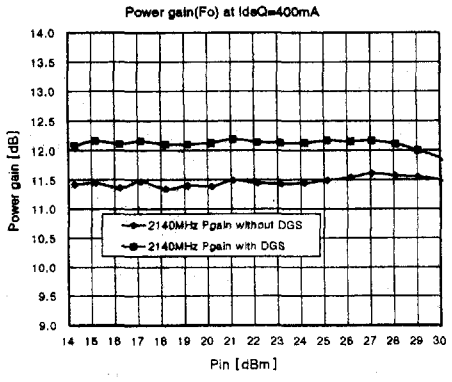

(c)

Fig. 4. Performance improvement by DGS for IdsQ of 400 mA. (a) the fundamental output power and PAE, (b) the second harmonic power, (c) power gain.

dramatic as shown in Fig. 4 (b). The remarkable improvement, i.e. the reduction, of 2Fo is observed. Through the rejection property of DGS at the second harmonic frequency as shown in Fig. 2 (b), the 2Fo component generated by the power device is reflected back to the device. Therefore, the detected 2Fo component after DGS line is surely reduced. The improvement of power gain by DGS is shown in Fig. 4 (c).

In order to investigate the performance improvement by DGS, the power amplifier was measured under various operating classes by adjusting IdsQ. The operating class is simply called class B in this work when IdsQ is 50 mA, although it is slightly higher point than the ideal class B. The IdsQ was also adjusted to be 1,000 mA, which is the current for the operating condition far beyond normal class A. The recommended IdsQ of 400 mA is called class AB in this work for convenience, although it is between normal class AB and A. The performance improvement by DGS under the three IdsQs has been verified through the measurement with input power swept.

Fig. 5 (a) ~ (c) show the observed performance for the two cases. To make the figures brief and readable, the measured results are illustrated here only for three inputs, 20 dBm, 27 dBm, and 30 dBm, and the three IdsQs. From Fig. 5 (a), it is evident that the output power of "WITH DGS" is greater than that of "WITHOUT DGS" for all operating classes. The improvement of output power leads to improved power added efficiency, as shown in Fig. 5 (c). It is also definite, from Fig. 5 (b), that the second harmonic component of "WITH DGS" is much smaller than that of "WITHOUT DGS" for all classes.

Fig. 6 (a)~(c) show the measured data for the two cases in order to quantify the improvement by DGS. The output power has been improved by 0.16~0.65 dBm, 0.37~0.75 dBm, and 0.14~0.68 dBm for 50 mA, 400 mA, and 1,000 mA of IdsQ respectively. Considerable differences in the magnitude of 2Fo between "WITH DGS" and "WITHOUT DGS" for each class is observed from Fig. 6 (b). It is observed that the reduction of 2Fo for 50 mA and 400 mA are outstanding compared to 1,000 mA. The resultant PAEs of "WITH DGS" are greater than that of "WITHOUT DGS" by 0.4~1.92 %, 0.56~3.39 %, and 0.41 ~2.65 %, respectively.

It is meaningful to review the measured performance and improvement in the measured results described above. The rejection of the second harmonic of class B is greater than in the other classes, because as is expected, the distortion of the signal is much more severe than in the other classes. However, the increase in fundamental output power of class B is smaller than other classes. This can be explained by considering that the output power of class B is generally the smallest for the same input power, thus the quantity of improvement is relatively small than the other classes.

The magnitude of the third harmonic for the two cases have

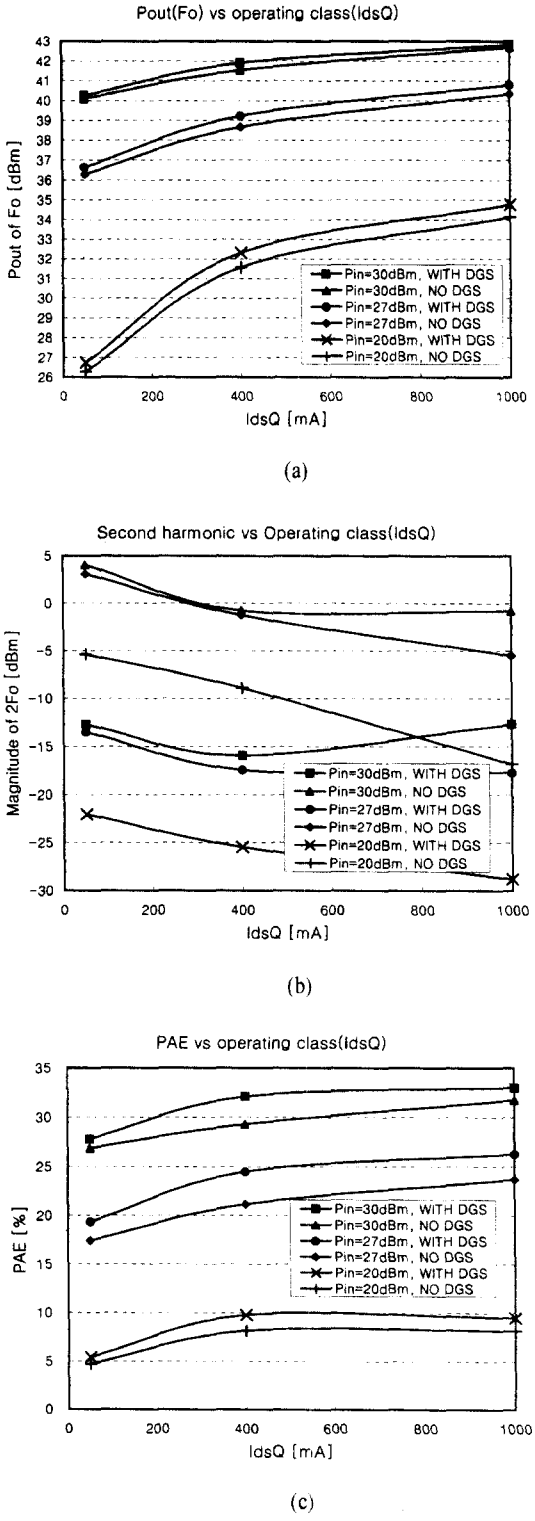

Fig. 5. Performance improvement by DGS for various operating classes by adjusting IdsQ. (a) the fundamental output power, (b) the second harmonic power, (c) power added efficiency.

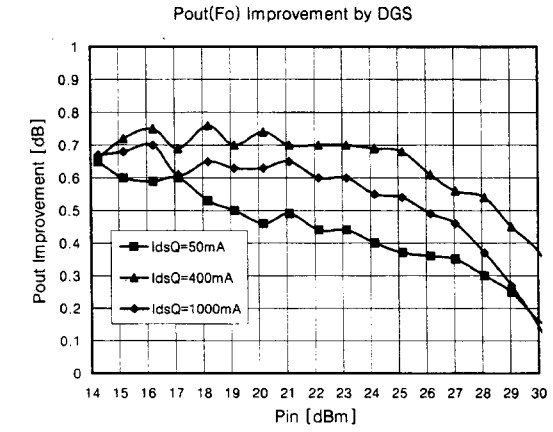

(a)

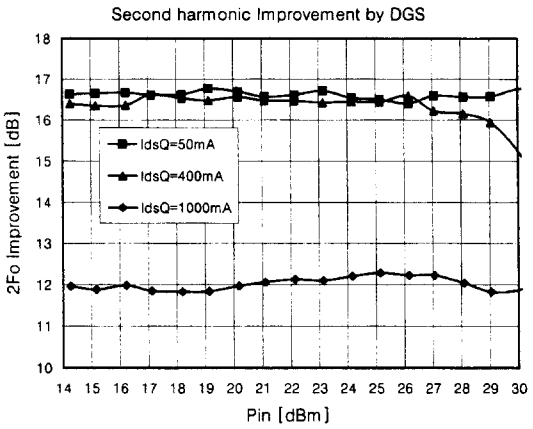

(b)

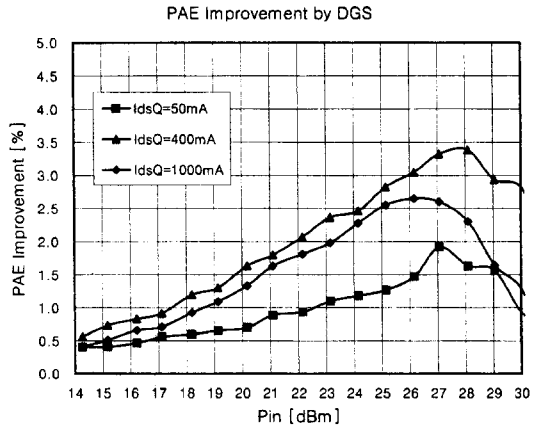

(c)

Fig. 6. The quantities of improvement by DGS under various operating classes by adjusting IdsQ. (a) the fundamental output power, (b) the second harmonic power, (c) power added efficiency.

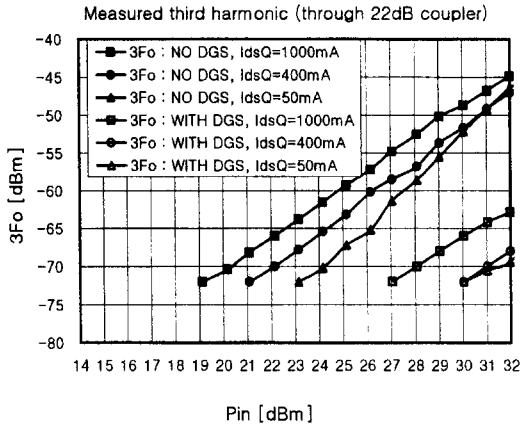

Fig. 7. The measured third harmonic component through 22dB coupler.

also been measured and compared in Fig. 7. The improvement of the third harmonic amounts to around 20 dB. A 22dB-coupler at the third harmonic frequency has been used in detecting the third harmonic. The measured third harmonic under −72 dBm is truncated in Fig. 7, because it was difficult to identify the exact magnitude of the detected power less than −72 dBm on the screen of our spectrum analyzer. The true magnitude of the third harmonic can be calculated easily by adding 22 dB to Fig. 7. Anyway, the improvement of the third harmonic component is also observed definitely.

Ⅳ. Two-Tone Measurement and IMD3 Improvement by DGS

In the above section, it has been described that the improvement in output power, harmonic rejection, and power added efficiency could be obtained at all operating classes by DGS. Based on the improvements in 1-tone power measurement, we are going to show the reduction of IMD3. Fig. 8 represents the generally used, simplified nonlinear circuits for the analysis of IMD3[11],[12]. Using the basic circuit concepts, it is possible to define the current source, internal equivalent impedance, and nonlinear resistive and reactive loads. The components of the nonlinear current can be expressed like eq. (1). In a linear or weakly nonlinear region, G_2 and C_2 are dominant over G_3 and C_3.

$$i_{NL}(t) = \left[G_2 + \frac{\partial}{\partial t}C_2\right]v^2(t) + \left[G_3 + \frac{\partial}{\partial t}C_3\right]v^3(t) \quad (1)$$

When the input and output are $i_s(t)$ and $v(t)$ respectively, the Volterra nonlinear transfer functions up to the third order can be expressed as eqs. (2)~(4).

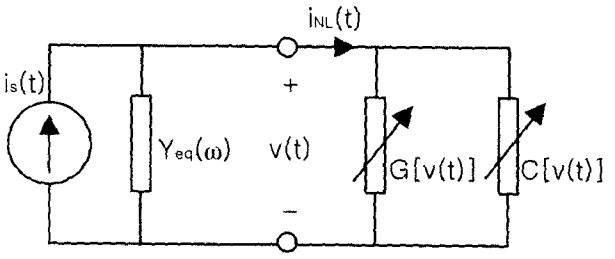

Fig. 8. Simplified nonlinear circuit for IMD analysis.

$$H_1(\omega)=\frac{1}{Y_{eq}(\omega)}=Z_{eq}(\omega) \tag{2}$$

$$H_2(\omega_1,\omega_2)=-Z_{eq}(\omega_1+\omega_2)\{G_2+j(\omega_1+\omega_2)C_2\}[H_1(\omega_1)H_1(\omega_2)] \tag{3}$$

$$H_3(\omega_1,\omega_2,\omega_3)=\frac{-Z_{eq}(\omega_1+\omega_2+\omega_3)}{6}\left\{\begin{array}{l}2\{G_2+j(\omega_1+\omega_2+\omega_3)C_2\}\left[\begin{array}{l}H_1(\omega_1)H_2(\omega_2,\omega_3)\\+H_1(\omega_2)H_2(\omega_1,\omega_3)\\+H_1(\omega_3)H_2(\omega_2,\omega_1)\end{array}\right]\\+6\{G_3+j(\omega_1+\omega_2+\omega_3)C_3\}[H_1(\omega_1)H_1(\omega_2)H_1(\omega_3)]\end{array}\right\} \tag{4}$$

Eqs. (3) and (4) can be rewritten for a 1-tone input signal as follows ;

$$H_2(\omega,\omega)=-Z_{eq}(2\omega)\{G_2+j2\omega C_2\}[H_1^2(\omega)] \tag{5}$$

$$H_3(\omega,\omega,\omega)=\frac{-Z_{eq}(3\omega)}{6}\left\{\begin{array}{l}2\{G_2+j(3\omega)C_2\}[3H_1(\omega)H_2(\omega,\omega)]\\+6\{G_3+j(3\omega)C_3\}[H_1^3(\omega)]\end{array}\right\} \tag{6}$$

Provided that 2-tone input signals, w_1 and w_2, are injected into the power amplifier with the same magnitude, it is possible to express the input signal as $i_s(t)=e^{j\omega_1 t}+e^{j\omega_2 t}$. At frequencies $(2w_2-w_1)$ and $(2w_1-w_2)$, the IMD3 components can be modeled as eqs. (7-a) and (7-b).

For $(2w_1-w_2)$,

$$H_3(\omega_1,\omega_1,-\omega_2)=\frac{-Z_{eq}(2\omega_1-\omega_2)}{6}\left\{\begin{array}{l}2\{G_2+j(2\omega_1-\omega_2)C_2\}\left[\begin{array}{l}H_1(-\omega_2)H_2(\omega_1,\omega_1)\\+2H_1(\omega_1)H_2(-\omega_2,\omega_1)\end{array}\right]\\+6\{G_3+j(2\omega_1-\omega_2)C_3\}[H_1^2(\omega_1)H_1(-\omega_2)]\end{array}\right\} \tag{7-a}$$

, and for $(2w_2-w_1)$,

$$H_3(\omega_2,\omega_2,-\omega_1)=\frac{-Z_{eq}(2\omega_2-\omega_1)}{6}\left\{\begin{array}{l}2\{G_2+j(2\omega_2-\omega_1)C_2\}\left[\begin{array}{l}H_1(-\omega_1)H_2(\omega_2,\omega_2)\\+2H_1(\omega_2)H_2(-\omega_1,\omega_2)\end{array}\right]\\+6\{G_3+j(2\omega_2-\omega_1)C_3\}[H_1^2(\omega_2)H_1(-\omega_1)]\end{array}\right\} \tag{7-b}$$

It can be said that the magnitudes of $H_2(w, w)$ and $H_3(w, w, w)$ have been reduced by DGS because of the decreased second and third harmonics. Considering eqs. (5) and (6), the reduction is directly related to the reduction of G_2, C_2, G_3, and C_3, though it can be said that $H_1(w)$ has been increased because of the improved output power. However, it is concluded that the relative reduction of G_2, C_2, G_3, and C_3 is dominant over the relative increase of $H_1(w)$, because $H_2(w, w)$ and $H_3(w, w, w)$ have been reduced.

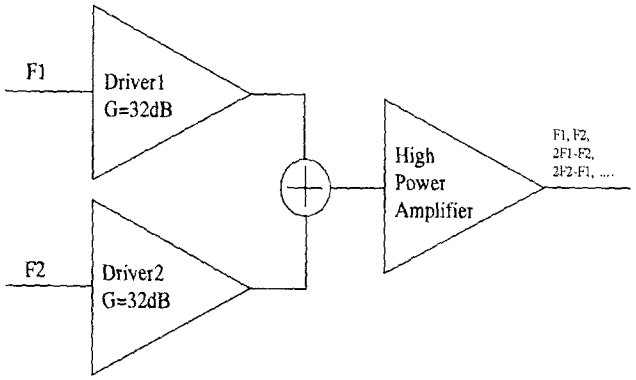

Fig. 9. Test setup for the 2-tone measurement.

Now, the improvement of IMD3 by DGS can be described using eqs. (1), (5), (6), (7-a), and (7-b). In (7-a) and (7-b), the third order nonlinear transfer functions are strongly dependent on G_2, C_2, G_3, C_3, $H_1(.)$, and $H_2(.\ ,\ .)$. The harmonic rejection decreases not only G_2 and C_2, but also G_3 and C_3. In addition, $H_2(.\ ,\ .)$ has been reduced quitely despite the relatively slight increase of $H_1(.)$. Therefore, in (7-a) and (7-b), it can be said that the relative reductions of G_2, C_2, G_3, C_3, and $H_2(.\ ,\ .)$ are also dominant over the relative increase of $H_1(.)$.

Fig. 9 shows the 2-tone test setup briefly. Two driver amplifiers whose gain and power performance are almost identical are placed in front of a power combiner for the generation of enough input signals. The third-order intermodulation distortion components have been measured for the two cases with two input signals swept from −21 to −3 dBm/tone.

Fig. 10 (a)~(c) show the measured IMD3 performance under the IdsQs of 50 mA, 400 mA, and 1,000 mA. The IMD sweep spot, which is the typical phenomenon of class B operation, is observed in Fig. 10 (a). The IMD3 improvement by DGS is observed for all operating classes as has been expected through the nonlinear transfer functions and the related description above. The improved measures of IMD3 under all IdsQs are summarized in Fig. 11.

It is interesting to compare the IMD3 improvement vs. operating class. Fig. 11 shows that the IMD3 improvement under the IdsQ of 400 mA is better than the other classes. In this class, maximum 4dB of improvement has been achieved by DGS, while the maximum improvement under IdsQs of 50 mA and 1,000 mA are 2.2 dB and 1.3 dB respectively. If the sweep spot region is excluded, the maximum improvement is 0.7 dB for the case of IdsQ of 50 mA.

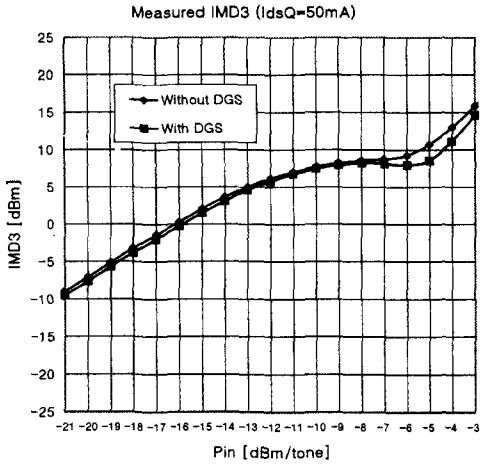

(a)

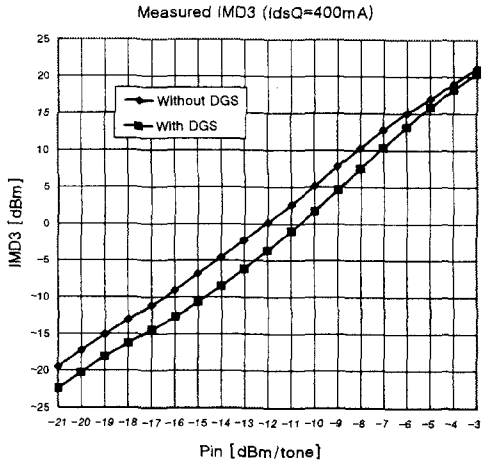

(b)

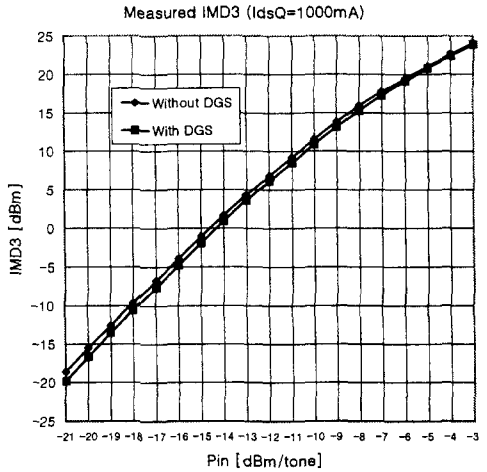

(c)

Fig. 10. IMD3 improvement by DGS for various IdsQs. (a) 50 mA, (b) 400 mA, (c) 1,000 mA.

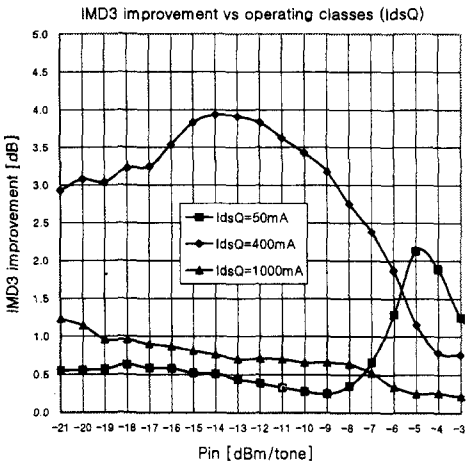

Fig. 11. Quantities of IMD3 improvement by DGS for various operating classes by adjusting IdsQ.

Before discussing the differences depending on class, some considerations should be noted first ; 1) The fundamental output power under IdsQ of 50 mA is the smallest, while the distortion is the most severe. 2) The normal class A operation produces the highest output power with the smallest distortion. 3) In this work, the IdsQ of 1,000 mA is a much higher operating point than normal class A. As there is no distortion in normal class A operation theoretically, the swing of the input signal goes into distortion again as the input power increases and gets closer tothe saturation point when the IdsQ is 1,000 mA. 4) Because G_2, C_2, G_3, and C_3 are strongly bias dependent, they are smaller in normal class A or AB than class B or far beyond class A, except for low level of input swing.

Now, IMD3 improvement for different operating classes can be explained by relating these four considerations to eq. (7-a) or (7-b). Even though G_2, C_2, G_3, and C_3 have been reduced by DGS, the relative magnitudes of G_2, C_2, and $H_2(.\ ,\ .)$ at the IdsQ of 50 mA are still higher than the other classes as shown in Fig. 5(b). Therefore, the first term in eq. (7-a), $2[G_2 + j(2\omega_1 - \omega_2)C_2]$ $[H_1(-\omega_2)H_2(\omega_1,\omega_1) + 2H_1(\omega_1)H_2(-\omega_2,\omega_1)]$, is still dominant in determining IMD3. Hence, it is understood that the relative improvement of IMD3 at the IdsQ of 50 mA is smaller than 400 mA as shown in Fig. 11.

It may be expected that the IMD3 improvement at the IdsQ of 1,000 mA should be better than or equal to that at 400 mA at least according to the description above. However, contrary to this expectation, the IMD3 improvement at 1,000 mA shown in Fig. 11 is poorer than 400 mA. The reason is that the IdsQ of 1,000 mA is not the quiescent condition of normal class A, but is far beyond class A. It seems that the distortion at 1,000 mA is more severe than that at 400 mA from Fig. 5(b). The obtained improvement of IMD3 at 1,000 mA shown in Fig. 11 gives us

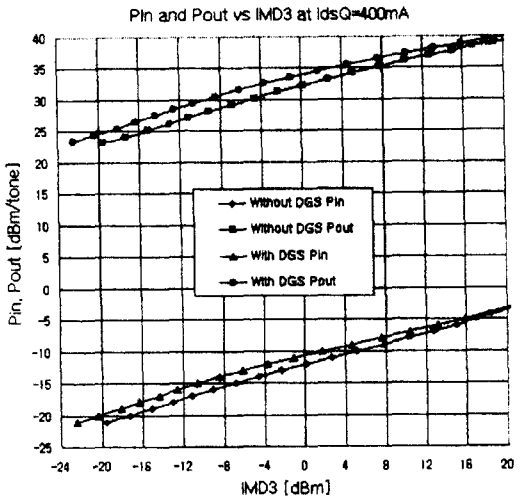

Fig. 12. Comparison of Pin and Pout for the same magnitude of IMD3, which shows the improvement of linearity.

one clue related to the operating classes. The improvement degrades slightly as the input goes up. This is due to the accelerated increase of distortion with the increase of input power. This verifies that the IdsQ of 1,000 mA is beyond the quiescent current of normal class A.

It is significant to compare the input and output power for the same level of IMD3, because this is one of the barometers for the linearity of power amplifiers, especially in digital communication systems. In other words, as high an input and output as possible for the same magnitude of IMD3 are required for good linearity. Fig. 12 represents the better linearity of "WITH DGS" than "WITHOUT DGS" in class AB. It can be read definitely that the required input and output in the case of "WITH DGS" are greater than "WITHOUT DGS" for a specified IMD3. Hence the power amplifier with DGS can perform the more linear operation.

V. Conclusion

A new method for improving the performance of power amplifiers by tuning the harmonic components using DGS has been presented. The measured performance parameters such as output power, power added efficiency, harmonic rejection, and IMD3 were discussed for two cases ; the power amplifier with and without DGS section attached at the output section. It was verified that 1) a microstrip line with DGS on the ground plane has a very wide stopband and can be used for tuning harmonics in power amplifiers, and 2) harmonic rejection by DGS plays an important role in improving the performance of power amplifiers under various operating classes.

The differences in the improvement of IMD3 for different operating classes were also described using a simplified equivalent nonlinear circuit and related nonlinear transfer functions. In order to clarify that the IMD3 improvement differs depending on the operating classes, two kinds of amplifier, one is adopting a 30 Watts device, the other a small signal device, were measured. The IMD3 improvement under normal class A was relatively better than the other classes. However, if the IdsQ increases beyond normal class A. the improvement is degraded.

The DGS line is separated from the power amplifier intentionally in this work, because, to our knowledge, this is the first attempt to improve the performance of a power amplifier of a few tens Watt-level using DGS under various operating classes. Therefore, it was essential to measure and compare the performance for two cases, "WITH DGS" and "WOTHOUT DGS". However, it is easily possible to incorporate DGS patterns under the 50-Ω connection line after the output matching network and DC block. It is expected that the technique in this work are well applicable with no limits in MMIC power amplifiers, although the performance improvement of the power amplifier by DGS has been achieved using hybrid MIC technology here.

This work was supported by the Brain Korea 21 Project.

References

[1] J. L. B. Walker, *High-Power GaAs FET Amplifiers*, pp. 210-212, Artech House, MA, 1993.

[2] S. C. Cripps, *RF Power Amplifiers for Wireless Communications*, pp. 88-90, Artech House, MA, 1999.

[3] S. Mazumder, A. Azizi, and F. Gardiol, "Improvement of a Class-C Transistor Power by The second-Harmonic Tuning", *IEEE Trans. Microwave Theory Tech.*, vol. MTT-27, no. 5, pp.430-433, May 1979.

[4] J. Lane, R. Freitag, H. -K. Hahn, J. Degenford, and M. Cohn, "High-Efficiency 1-, 2-, and 4-W Class-B FET Power Amplifiers", *IEEE Trans. Microwave Theory Tech.*, vol. MTT-34, no. 12, pp. 1318-1826, Dec. 1986.

[5] C. Duvanaud, S. Dietsche, G. Pataut, and J. Obregon, "High-efficiency class F GaAs FET amplifier operating with very low bias voltage for use in mobile telephones at 1.75GHz", *IEEE Microwave Guide Wave Lett.*, vol. 3, pp. 268-270, Aug. 1993.

[6] E. Camargo, and R. M. Steinberg, "A compact high power amplifier for handy phones", *1994 IEEE MTT-S Digest*, pp. 565-568, 1994.

[7] V. Radisic, Y. Qian, and T. Itoh, "Broad power amplifier using dielectric photonic bandgap structure," *IEEE Micro-*

wave Guide Wave Lett., Zvol. 8, pp. 13-14, Jan. 1998.

[8] J. S. Lim, H. S. Kim, J. S. Park, D. Ahn, and S. Nam, "A Power Amplifier with Efficiency Improved Using Defected Ground Structure", *IEEE Microwave and Wireless Component Lett.*, vol. MWCL-11, No. 4, pp. 170~172, Apr. 2001.

[9] C. S. Kim, J. S. Park, D. Ahn and J. B. Lim, "A Novel 1-D Periodic Defected Ground Structure for Planar Circuits", *IEEE Microwave Guide Wave Lett.*, vol. 10, pp.131-133, Apr. 2000.

[10] D. Ahn, J.-S. Park, C.-S. Kim, J. Kim, , Y. Qian, and T. Itoh, "A Design of the Low-Pass Filter Using the Novel Microstrip Defected Ground Structure", *IEEE Trans. Microwave Theory Tech.*, vol. 49, No. 1, pp. 86-93, Jan. 2001.

[11] S. A. Maas, Nonlinear Microwave Circuits, pp.172-199, Artech House, MA, 1988.

[12] N. B. Carvalho and J. C. Pedro, "Two-Tone IMD Asymmetry in Microwave Power Amplifiers", *2000 IEEE MTT-S Digest*, pp.445-448, Jun 2000.

Jong-Sik Lim

was born in Hwasun, Korea. He received the B.S., M.S. degrees in electronic engineering from Sogang University, Seoul, Korea, in 1991 and 1993, respectively. He joined Electronics and Telecommunications Research Institute (ETRI), Daejeon, Korea in 1993, and was with them for 6 years in Satellite Communications Division as a senior member of research staff. He was one of key members in developing MMIC LNA and SSPA for the 20/30 GHz satellite transponder in ETRI. Since 1999, he has been working toward the Ph. D. in the school of Electrical Engineering and Computer Science, Seoul National University. His current research interests include design of the passive and active circuits for RF/microwave and millimeter-wave with MIC/MMIC technology, modeling of active device, design of high power amplifiers for mobile communications, applications of periodic structure to the RF/microwave circuits and modeling of passive structure with periodic structure.

Jun-Seok Park

was born in Seoul, Korea, on August 12, 1969. He received the B.S. and M.S. degrees in electronic engineering from the Kookmin University, Seoul, Korea, in 1991 and 1993, respectively. In 1996, he received the Ph.D. degree from the Laboratory of RF & MMIC of the Kookmin University. In 1997, he joined the Department of Electrical Engineering at the University of California at Los Angeles as a Postdoctoral Researcher. In March 1998, he joined the Soonchunhyang University, Asan, Korea, as an Assistant Professor of electronic and electrical engineering. Also he is currently senior researcher of RF and microwave component research center (RAMREC), Soonchunhyang University, Asan, Korea. His research interests include electromagnetic field analysis and simulation, passive components, MCM-C, RF active devices as well as RF modules for Korea Cellular and PCS systems.

Young-Taek Lee

was born in Seoul, Korea, in 1975. He received the B.S. and the M.S. degrees in electrical engineering at the Seoul National University, Seoul, Korea, in 1998 and 2000, respectively, and is currently working toward the Ph.D. degree in Seoul National University. His research interests include analysis and design of low phase noise microwave oscillators, high Q resonator design, active/passive microwave circuits design.

Dal Ahn

was born in Kimje, Korea, on October 15, 1961. He received the B.S., M.S. and Ph.D degrees from the Sogang University, Seoul, Korea, in 1984, 1986, and 1990, respectively, all in electronics. From 1990 to 1992, he was with the Mobile Communications Division, Electronics and Telecommunications Research Institute, Daejeon, Korea. Since 1992, he has been with the School of electrical and electronic engineering, Soonchunhyang University, Asan, Korea, where he is currently a associate professor. Also he is currently Chief of RF and microwave component research center (RAMREC), Soonchunhyang University, Asan, Korea. His current research interests include the design and application of passive and active components at radio and microwave frequencies, and the circuit modeling using commercial electromagnetic analysis program. He is technical consultant of Tel Wave Inc., Suwon, Korea and MRW Technologies, Paju, Korea.

Jae-Hee Han

was born in Seoul, Korea, in 1970. He received the B.S. and M.S. degrees in electrical Engineering from the Seoul National University, Seoul, Korea, in 1996 and 1998, respectively, and is currently working toward the Ph.D. degree in Seoul National University. His interests include the design of microwave circuits and linearization techniques for high- power amplifiers.

Byung-Sung Kim

was born in Seoul, Korea, in 1965. He received the B.S, and Ph.D degrees in electronic engineering from Seoul National University in 1989 and in 1997, respectively. Since 1997, he has been with the School of Electrical and Computer Engineering, Sungkyunkwan University, Suwon, Korea, where he is currently an Assistant Professor. His current research interests include the modeling of RF active devices and the design of RFICs using SiGe HBT.

Sang-wook Nam

received the B.S. degree from the Seoul National University, Seoul, Korea, in 1981, the M.S. degree from the Korea Advanced Institute of Science and Technology, Seoul, Korea, in 1983, and the Ph.D. degree from the University of Texas at Austin, in 1989, all in electrical engineering. From 1983 to 1986, he was a researcher at Gold Star Central Research Laboratory, Seoul, Korea. Since 1990, he has been with Seoul National University, where he is currently a Professor in the School of Electrical Engineering. His research interests include analysis/design of electromagnetic (EM) structures, antennas and microwave active/passive circuits.